Morphological Behavior of A_5B Miktoarm Star Block Copolymers

Frederick L. Beyer and Samuel P. Gido*

Department of Polymer Science & Engineering, University of Massachusetts Amherst, Amherst, Massachusetts 01003

Gabriel Velis and Nikos Hadjichristidis

Department of Chemistry, University of Athens, Panepistimiopolis Zografou 15771, Athens, Greece

Nora Beck Tan

U. S. Army Research Laboratory, Aberdeen Proving Ground, Maryland 21005-5069

Received June 18, 1999

ABSTRACT: A morphological study of three A_5B, six-arm miktoarm star block copolymers is presented. The miktoarm stars are comprised of five arms of polyisoprene and one arm of polystyrene joined together at a single junction point. The strong segregation limit theory for the morphological behavior of miktoarm stars predicts that these materials should form cylindrical (two samples) and lamellar (one sample) morphologies, but only lamellar morphologies were observed by TEM and SAXS. These results are similar to previously reported discrepancies between miktoarm star morphological behavior and the predictions of the theory. Combining the data of this study with that of previous morphological studies of miktoarm star materials, we can track the increasing discrepancy between the experimentally observed morphology and theoretical predictions as the molecular asymmetry parameter, ϵ, increases. The A_5B materials in this study were also observed to form exceptionally well-ordered morphologies.

Introduction

Branched and grafted molecular architecture has been shown to be an additional factor (in addition to volume fraction and degree of segregation) that affects the morphological behavior of block copolymers. Guided by the predictions of a mean field theory derived by Milner[1,2] for the morphological behavior of A_nB_m-type, miktoarm star block copolymers, work has focused on molecules with an array of architectures including A_2B stars,[3−6] A_3B stars,[7] A_nB_n stars,[8−10] and multigraft architectures which may be considered to be linear combinations of miktoarm stars.[11−13] These studies have borne out the predictions of the model in general but have revealed systematic discrepancies. The purpose of this study is to examine A_5B miktoarm star block copolymers, whose architecture is illustrated in Figure 1. These materials have the highest architectural asymmetries investigated thus far.

In the current work, three A_5B miktoarm stars of polyisoprene (PI) and polystyrene (PS) have been characterized. Their bulk morphology is predicted by the Milner theory, which is strictly applicable only in the strong segregation limit. Figure 2 shows the morphology diagram generated by this model. For architecturally and conformationally asymmetric block copolymer stars of type A_nB_m, the theory predicts morphology as a function of B component volume fraction, ϕ_B, and a molecular asymmetry parameter, $\epsilon = (n_A/n_B)(l_A/l_B)^{1/2}$. Here, n_A and n_B are the numbers of arms of block materials A and B, and $l_i = (V_i/R_i^2) = v_i/b_i^2$. V_i and R_i are the volume and radius of gyration of one arm of polymer i, while v_i is the segmental volume and b_i the statistical segment length of component i.

The materials in this study, A_5B stars of PI and PS, have five arms of PI and one arm of PS per molecule, joined to each other at a single junction point. Using segmental volumes of 132 Å^3 (PI) and 176 Å^3 (PS) and Kuhn lengths of 6.8 Å (PI) and 6.9 Å (PS), an ϵ of 4.4 is calculated for these materials.[14,15] The samples characterized have PS volume fractions of 0.60 (I_5S-1), 0.67 (I_5S-2), and 0.77 (I_5S-3).

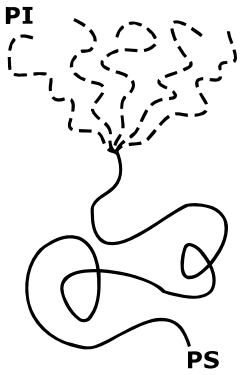

Figure 1. Illustration of the molecular architecture of an A_5B miktoarm star block copolymer. In this study, the A_5B stars are comprised of five PI arms and one PS arm joined at a single junction point.

Experimental Section

Three A_5B miktoarm stars of PI and PS were synthesized using anionic polymerization and controlled chlorosilane chemistry. The synthesis of the A_5B stars has been described in detail elsewhere.[16] All manipulations were performed in glass reactors under high vacuum. The reactors were previously washed with benzene solution of *n*-butyllithium and rinsed with benzene. Benzene was the solvent for all polymerizations and linking reactions. The PS and PI arms were synthesized separately using *sec*-butyllithium as initiator and then linked together with the hexafunctional chlorosilane 1,2-bis(trichlorosilyl)ethane.

Table 1 lists the molecular characteristics of each sample. Membrane osmometry (MO) was performed in toluene at 35

* To whom all correspondence should be addressed.

10.1021/ma9909713 CCC: $18.00
Published on Web 09/11/1999

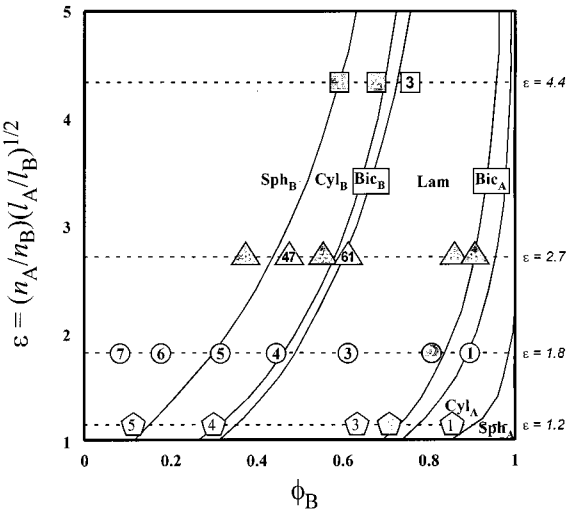

Figure 2. Morphology diagram generated by the Milner model. Morphology is given for the volume fraction of the B component, ϕ_B, and molecular asymmetry, ϵ. The A_5B stars are represented by squares while A_2B stars are represented by circles, A_3B stars by triangles, and A_2B_2 stars by pentagons. Shaded symbols indicate a sample whose morphology disagrees with that predicted by theory.

°C. Size-exclusion chromatography with both refractive index (SEC) and UV (UV−SEC) detectors (λ = 262 nm) was performed in tetrahydrofuran (THF) at 30 °C. Vapor pressure osmometry (VPO) was performed in toluene at 50 °C. Proton nuclear magnetic resonance (^{1}H NMR) was used to determine the weight fraction of PS in each sample. Finally, the weight fraction of PS in each sample was calculated by dividing the PS arm M_n, as measured by SEC, by the total M_n of the star, $M_n(\mu) = 5(M_n(\text{PI})) + M_n(\text{PS})$. The volume fraction PS was calculated for each sample using the mass percent of PS measured by ^{1}H NMR and bulk densities.[17]

Bulk films were cast from 4 wt % solution in toluene, a nonselective solvent for PI and PS.[18] Films approximately 2 mm thick were formed by allowing the solvent to evaporate slowly over a period of 2 weeks. The films were left standing at room temperature and atmospheric pressure for an additional week and then placed under vacuum at room temperature for 1 week to remove any residual solvent from the bulk material. The samples were subsequently annealed under vacuum for 1 week at 120 °C. The samples were then cooled under vacuum to room temperature over a period of several hours.

Table 1. Molecular and Morphological Characterization Information for the Three I_5S Miktoarm Stars

			I_5S-1	I_5S-2	I_5S-3
PS arm	M_n (g/mol)	MO	76000	106000	167500
	PDI	SEC	1.02	1.03	1.03
PI arm	M_n (g/mol)	VPO	10400	9700	9700
	PDI	SEC	1.03	1.04	1.04
miktoarm star	M_n (g/mol)	MO	126000	152000	218000
	M_n (g/mol)	calc	128000	154500	216000
	PDI	SEC	1.05	1.05	1.05
	mass % PS	^{1}H NMR	63	70	79
	mass % PS	UV-SEC	61	67	75
	mass % PS	calc	60	69	77
	vol % PS	calc	59.9	67.2	76.8
	q^* (Å^{-1})		0.0147	0.0131	0.0099
	d (Å)		427	479	629
	predicted morphology		C	C	L
	observed morphology		L	L	L

Sample morphology was characterized using a combination of transmission electron microscopy (TEM) and small-angle X-ray scattering (SAXS). To prepare thin sections for microscopy, a Leica Ultracut UCT microtome equipped with a Leica EM FCS cryogenic sample chamber operated at −110 °C was used to cut sections approximately 500 Å in thickness. The sections were collected on TEM grids and stained 4 h in OsO_4 vapor. A JEOL 100CX TEM, operated at an accelerating voltage of 100 kV, was used to image the stained sections. SAXS data were collected at the Advanced Polymers Beamline (X27C), located at the National Synchrotron Light Source at Brookhaven National Labs (BNL), Upton, NY. Two-dimensional scattering patterns were collected on Fujitsu image plates and then read by a Fujitsu BAS 2000 image plate reader. Custom software at BNL was used to subtract back-

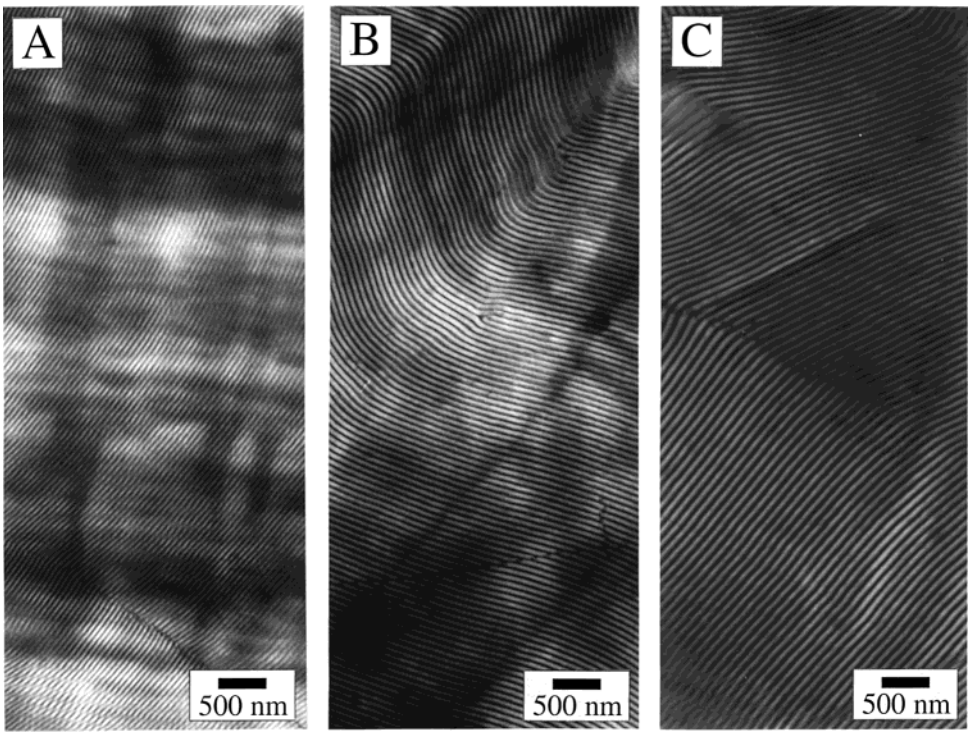

Figure 3. TEM micrographs of samples (a) I_5S-1, (b) I_5S-2, and (c) I_5S-3. All three samples formed lamellar morphologies.

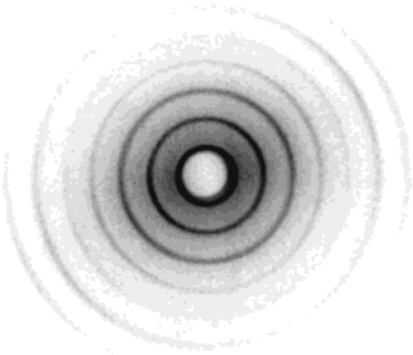

Figure 4. Two-dimensional SAXS data collected for sample I_5S-3, illustrating the unusual degree of long-range order present in these materials.

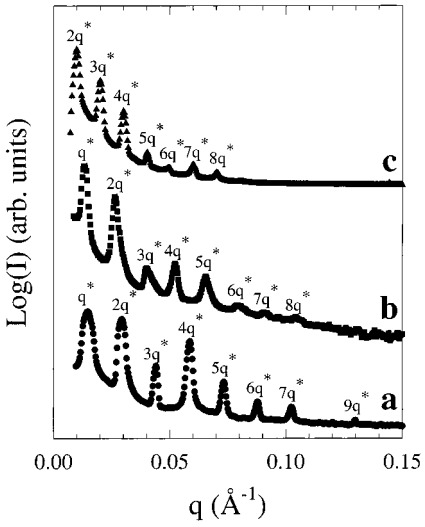

Figure 5. One-dimensional, log(*I*) vs *q* SAXS data for (a) I_5S-1, (b) I_5S-2, and (c) I_5S-3.

ground noise and perform circular averaging. Data were collected for a wavelength of 1.307 Å and a camera length of 1410 mm.

Results

The results of the morphological characterization for the three I_5S materials are collected in Table 1. Representative TEM micrographs indicating that all three samples (I_5S-1, I_5S-2, and I_5S-3) form lamellar morphologies are shown in Figure 3. A two-dimensional SAXS pattern collected for sample I_5S-3 is shown in Figure 4. Circularly averaged, one-dimensional SAXS data for all three samples are shown in Figure 5. The remarkable long-range order exhibited by these materials results in 8 or 9 orders of the lamellar repeat, with the scattering vectors of the peaks occurring at integral multiples of the scattering vector of the primary reflection (q^*), as expected for lamellae. In the SAXS data for I_5S-3, the primary reflection is obscured by the beam stop, and thus the first observed peak is at $2q^*$. The values of q^* for I_5S-1 and I_5S-2 were found to be 0.0147 and 0.0131 Å^{-1}, corresponding to lamellar long periods of 427 and 479 Å, respectively. Using the observed reflections for I_5S-3, q^* is calculated to be 0.0099 Å^{-1}, corresponding to a lamellar repeat of 635 Å.

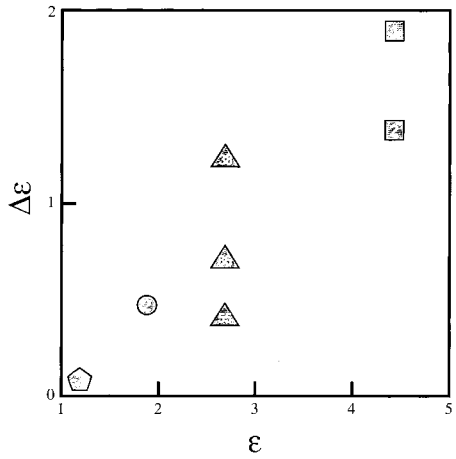

Figure 6. Values of $\Delta\epsilon$ for samples exhibiting morphologies other than those predicted by theory, as a function of ϵ, for the data shown in Figure 2. As in Figure 2, A_5B stars are represented by squares, A_2B stars by circles, A_3B stars by triangles, and A_2B_2 stars by pentagons.

Discussion

In addition to samples from three previous works involving A_2B, A_3B, and A_2B_2 miktoarm star block copolymers,[5,7,9] the three samples characterized in this paper are plotted on the morphology diagram in Figure 2. Those samples reported to have morphological behavior differing from their predicted morphologies are shaded. This figure reveals an increase in the frequency of discrepancies between predicted and observed behaviors with increasing molecular asymmetry. As indicated in Figure 2, the Milner model predicts that only one of the three I_5S samples, I_5S-3, has the correct volume fraction of PS to exhibit a lamellar morphology. Both samples I_5S-1 and I_5S-2 are predicted to form cylinders of PS but are found experimentally to form lamellae. This discrepancy is in agreement with the general trend observed in prior studies which tested lower ϵ portions of the morphology diagram.

As with previous studies, samples that disagree with theoretical predictions exhibit morphologies that should occur at lower ϵ for a given ϕ_B or at a higher ϕ_B for a given ϵ. For example, Tselikas et al.[7] found that their I_3S-55 sample formed lamellae instead of the predicted cylinders of PS. While ϵ for I_3S-55 was calculated to be approximately 2.7, for the same volume fraction, lamellae occur at a maximum of $\epsilon \approx 2.2$. Alternately, for $\epsilon = 2.7$, lamellae are predicted to occur for ϕ_B greater than 0.6 but are observed at ϕ_B of 0.55. If similar comparisons are made for all the samples that disagree with the theory, one finds that the overestimation of morphological shift increases with asymmetry; slight discrepancies at low values of ϵ become greater as asymmetry increases. This is represented graphically in Figure 6, which shows a plot of $\Delta\epsilon$ as a function of increasing ϵ, where $\Delta\epsilon$ is the negative shift in ϵ required to bring a sample into agreement with the diagram. The I_3S-55 sample, for example, would have a $\Delta\epsilon$ of $2.7-2.2 = 0.5$. Plotted as a function of ϵ, the maximum in this shift increases with ϵ. These trends can only be represented approximately given the limited experimental data available; i.e., the data points available do not necessarily represent the limits of the discrepancy between theory and experiment at each value of ϵ.

Conclusions

As seen in prior studies, the Milner theory exhibits a systemic tendency to overestimate the effect of architectural molecular asymmetry of block copolymer morphology. This tendency becomes exaggerated with increasing asymmetry as in the I_5S samples of this study. Additionally, the three I_5S samples self-assembled to form remarkable long-range order in their lamellar morphologies as indicated by the unusual number of Bragg reflections observed in SAXS data.

Acknowledgment. The authors thank Dr. B. Hsiao, Dr. F.-J. Yang, Dr. J. Dietzel, and Ken Laverdure for their help in collecting SAXS data. This research was funded by the U.S. Army Research Office under Contracts DAAG55-98-1-0116 and DAAG55-98-1-0005. Central Facility support from the Materials Research Science and Engineering Center (MRSEC) at the University of Massachusetts—Amherst as well as the W. M. Keck Electron Microscopy Laboratory is also acknowledged. G.V. and N.H. thank the Exxon Research and Engineering Co., NJ, and the Research Committee of the University of Athens for their financial support.

References and Notes

(1) Milner, S. T. *Macromolecules* **1994**, *27*, 2333.
(2) Olmsted, P. D.; Milner, S. T. *Macromolecules* **1998**, *31*, 4011.
(3) Hadjichristidis, N.; Iatrou, H.; Behal, S. K.; Chludzinski, J. J.; Disko, M. M.; Garner, R. T.; Liang, K. S.; Lohse, D. J.; Milner, S. T. *Macromolecules* **1993**, *26*, 5812.
(4) Matsushita, Y.; Noda, I. *Macromol. Symp.* **1996**, *106*, 251.
(5) Pochan, D. J.; Gido, S. P.; Pispas, S.; Mays, J. W.; Ryan, A. J.; Fairclough, J. P. A.; Hamley, I. W.; Terrill, N. *Macromolecules* **1996**, *29*, 5091.
(6) Gido, S. P.; Lee, C.; Pochan, D. J.; Pispas, S.; Mays, J. W.; Hadjichristidis, N. *Macromolecules* **1996**, *29*, 7022.
(7) Tselikas, Y.; Iatrou, H.; Hadjichristidis, N.; Liang, K. S.; Mohanty, K.; Lohse, D. J. *J. Chem. Phys.* **1996**, *105*, 2456.
(8) Beyer, F. L.; Gido, S. P.; Poulos, Y.; Avgeropoulos, A.; Hadjichristidis, N. *Macromolecules* **1997**, *30*, 2373.
(9) Beyer, F. L.; Gido, S. P.; Uhrig, D.; Mays, J. W.; Beck Tan, N.; Trevino, S. F. Submitted to *J. Polym. Sci., Part B: Polym. Phys.*
(10) Turner, C. M.; Sheller, N. B.; Foster, M. D.; Lee, B.; Corona-Galvin, S.; Quirk, R. P.; Annis, B.; Lin, J.-S. *Macromolecules* **1998**, *31*, 4372.
(11) Lee, C.; Gido, S. P.; Poulos, Y.; Hadjichristidis, N.; Beck Tan, N.; Trevino, S. F.; Mays, J. W. *Polymer* **1998**, *39*, 4631.
(12) Lee, C.; Gido, S. P.; Poulos, Y.; Hadjichristidis, N.; Beck Tan, N.; Trevino, S. F.; Mays, J. W. *J. Chem. Phys.* **1997**, *107*, 6460.
(13) Xenidou, M.; Beyer, F. L.; Gido, S. P.; Hadjichristidis, N.; Beck Tan, N. *Macromolecules* **1998**, *31*, 7659.
(14) Gehlsen, M. D.; Bates, F. S. *Macromolecules* **1994**, *27*, 3611.
(15) Lin, C. C.; Jonnalagadda, S. V.; Kesani, P. K.; Dai, H. J.; Balsara, N. P. *Macromolecules* **1994**, *27*, 7769.
(16) Velis, G.; Hadjichristidis, N. *Macromolecules* **1999**, *32*, 534.
(17) *Polymer Handbook*, 3rd ed.; Wiley-Interscience: New York, 1989.
(18) Cowie, J. M. G. In *Developments in Block Copolymers - 1*; Goodman, I., Ed.; Applied Science Publishers: New York, 1982; p 1.

MA9909713